

# Foaming in stout beers

W. T. Lee\* and M. G. Devereux

MACSI, Department of Mathematics and Statistics, University of Limerick, Ireland.

We review the differences between bubble formation in champagne and other carbonated drinks, and stout beers which contain a mixture of dissolved nitrogen and carbon dioxide. The presence of dissolved nitrogen in stout beers gives them a number of properties of interest to connoisseurs and physicists. These remarkable properties come at a price: stout beers do not foam spontaneously and special technology, such as the widgets used in cans, is needed to promote foaming. Nevertheless the same mechanism, nucleation by gas pockets trapped in cellulose fibres, responsible for foaming in carbonated drinks is active in stout beers, but at an impractically slow rate. This gentle rate of bubble nucleation makes stout beers an excellent model system for the scientific investigation of the nucleation of gas bubbles. The equipment needed is very modest, putting such experiments within reach of undergraduate laboratories. Finally we consider the suggestion that a widget could be constructed by coating the inside of a beer can with cellulose fibres.

## I. INTRODUCTION

This paper describes the differences between foaming in drinks containing dissolved carbon dioxide (sparkling wines, carbonated beers and soft drinks) of which the most studied example is champagne, and stout beers. In this work, the term *stout beer* is taken not just to mean a “Very dark, full-bodied hopped beer”<sup>1</sup> but additionally one which foams due to a combination of dissolved nitrogen and carbon dioxide. Nitrogen is roughly 50 times less soluble in water than carbon dioxide and this affects the character of the bubbles and the foam in the head of the beer. One important difference is that while champagne and carbonated beers foam spontaneously, stout beers require special technology to promote foaming.

It has been shown theoretically and experimentally that stout beers do foam by the same mechanism as carbonated drinks, but that this occurs at rate too slow to generate a head in a feasible time. However, the gentle pace of bubble formation in stout beers make them an ideal system in which to investigate the physics of nucleation both for fundamental research and for undergraduate laboratory projects.

The rest of the article is divided up into the following sections. Section II summarises the relevant background physics: Henry’s law, Laplace’s law and nucleation barriers. Section III reviews the experimental evidence that the nucleation sites responsible for bubble formation in champagne and other carbonated drinks are cellulose fibres and describes a mathematical model of this nucleation process. Section IV discusses the unusual properties of stout beers, most of which be attributed to the low solubility of the nitrogen gas dissolved in the beers. Section V describes an extension of the mathematical model of bubble nucleation in champagne to the case of two gasses and its application to stout beers. The experimental observation of this bubbling mechanism is also described. The implications of these results to future investigations of the science of nucleation and new technologies for promoting foaming in canned and bottled stout beers are considered in section VI. Finally, conclu-

sions are given in section VII.

## II. BACKGROUND

In this section we summarise the background physics used in this paper, namely Henry’s law, which establishes an “exchange rate” between the concentration and partial pressure of dissolved gasses; Laplace’s law, which allows us to calculate the overpressure in a gas pocket trapped within a cellulose fibre; Fick’s first law, which relates the flux of a dissolved gas to its concentration gradient; and the nucleation barrier to bubble formation in a supersaturated gas solution. Values of parameters used in the text are summarised in Table I.

TABLE I. Parameters used in the calculations. A range of CO<sub>2</sub> pressures are used in carbonated beers. Here we assume that the total pressure in a carbonated beer is the same as in a stout beer.

Parameter	Value	Reference
$r$	$6.00 \times 10^{-6} \text{ m}$	2
$\lambda$	$14.00 \times 10^{-6} \text{ m}$	2
$\gamma$	$47.00 \times 10^{-3} \text{ N m}^{-1}$	2
$D_1$	$1.40 \times 10^{-9} \text{ m}^2 \text{ s}^{-1}$	
$D_2$	$2.00 \times 10^{-9} \text{ m}^2 \text{ s}^{-1}$	
$H_1$	$3.4 \times 10^{-4} \text{ mol m}^{-1} \text{ N}^{-1}$	
$H_2$	$6.1 \times 10^{-6} \text{ mol m}^{-1} \text{ N}^{-1}$	
$T$	293 K	
$P_0$	$1.00 \times 10^5 \text{ Pa}$	
Champagne		
$P_1$	$6.40 \times 10^5 \text{ Pa}$	4
Carbonated Beer		
$P_1$	$3.80 \times 10^5 \text{ Pa}$	
Stout Beer		
$P_1$	$0.80 \times 10^5 \text{ Pa}$	5
$P_2$	$3.00 \times 10^5 \text{ Pa}$	5

*a. Henry's Law* states that “when a gas dissolves the concentration of the (weak) solution is proportional to the gas pressure.”<sup>6</sup> Mathematically,  $c = HP$ , where  $c$  is the concentration of the dissolved gas in solution,  $P$  is the partial pressure of the gas in equilibrium with the solution and  $H$  is a constant of proportionality, the Henry's Law constant. Note that the units of  $c$  may be taken as  $\text{mol m}^{-3}$  (this work) or as  $\text{kg m}^{-3}$  and that Henry's law may also be stated as  $P = H'c$  (where  $H' = H^{-1}$ ) in textbooks. As noted in the definition, Henry's law only applies to weak (dilute) solutions, but it is valid for the range of pressures used in this paper.

*b. Laplace's Law* states that the pressure difference across a curved surface is equal to  $\gamma(R_1^{-1} + R_2^{-1})$  where  $\gamma$  is the surface tension of the interface and  $R_1$  and  $R_2$  are the principal radii of curvature of the interface.<sup>7</sup> For a spherical bubble of radius  $r$ ,  $R_1 = R_2 = r$  and the pressure,  $P_B$ , inside the bubble is given by

$$P_B = P_0 + \frac{2\gamma}{r}, \quad (1)$$

where  $P_0$  is atmospheric pressure. This expression is also valid for the pressure in a gas pocket trapped within a cellulose fibre, where  $r$  is taken to be the radius of the spherical caps at the ends of the gas pocket.

*c. Fick's First Law* describes the flux of a dissolved chemical. Fick's first law is that the flux  $Q$  is proportional to the gradient of the concentration,  $c$ , with constant of proportionality  $-D$

$$Q = -D\nabla c, \quad (2)$$

where, since  $D > 0$ , the minus sign ensures that the flux is directed from regions of high concentration to regions of low concentration.

*d. Critical Radius* Using Henry's law, Laplace's law and Fick's first law we can understand why there is a nucleation barrier to the growth of bubbles.<sup>6</sup> Consider a supersaturated gas solution in which the dissolved gas is at a concentration  $c = HP$ , where the pressure  $P$  of the gas in equilibrium with the solution is greater than atmospheric pressure  $P_0$ . Now consider the concentration of that dissolved gas  $c_B$  at the surface of a bubble. We expect this concentration to be in local equilibrium with the gas in the bubble

$$c_B = HP_B = H \left( P_0 + \frac{2\gamma}{r} \right). \quad (3)$$

In order for the bubble to grow, gas must flow from the bulk of the liquid into the bubble but, by Fick's first law, this will only occur if  $c > c_B$ . Inspection of equation 3 shows that this is not guaranteed simply because the solution is supersaturated,  $P > P_0$ , but a condition on the size of the bubble must also be met. The size of the bubble must exceed a critical radius  $r_C$  given by

$$r_C = \frac{2\gamma}{P - P_0}. \quad (4)$$

In other words, for champagne to effervesce and for beer to foam, bubbles larger than this critical radius must somehow be created. Bubbles for which  $r > r_C$  are known as post-critical nuclei. Note that the critical radius was derived using purely mechanical arguments, its value is a function only of the total pressure of dissolved gasses in solution independent of, for example, their solubility. In the subsequent sections we will discuss how this nucleation barrier is overcome in practise.

### III. BUBBLE NUCLEATION IN CHAMPAGNE

In this paper we take champagne as an example of a drink in which bubbles form due to dissolved carbon dioxide. This is because champagne is the most studied of all carbonated beverages, although the results described below are directly applicable to other carbonated drinks.

It has been known for some time that the spontaneous nucleation of bubbles in carbonated drinks is strongly inhibited.<sup>8</sup> As was discussed in the previous section, only bubbles above a critical radius will grow, and for gas pressures of less than one hundred atmospheres, the rate of spontaneous production of these post-critical bubbles either in bulk liquid or on surfaces in contact with the bulk liquid (suspended particles or the container walls) is practically zero.<sup>9</sup> Since the pressure of dissolved gasses in champagne is a little over six atmospheres this mechanism can be ruled out. Nevertheless, champagne and other carbonated drinks do produce bubbles so an alternative mechanism must be in play. This is now known to be the nucleation of bubbles by gas pockets. A gas pocket of post-critical size will grow due to diffusion of carbon dioxide from solution into the pocket. When the pocket exceeds some limiting size a bubble detaches, leaving behind the original, postcritical gas pocket. The process of growth and detachment repeats resulting in trains of bubbles rising to the surface. This is known as type IV nucleation.<sup>9</sup>

Until relatively recently it was thought that these gas pockets were held in imperfections on the surfaces of glasses. However, examination of the surface topography of glasses shows that the lengthscales of such imperfections are too small for gas pockets trapped within them to exceed the critical nucleus size. Microscopic observation of the sites on champagne glasses from which trains of bubbles emerge reveal that the gas pockets are trapped within cellulose fibres as shown in Figure 1.<sup>10</sup> The cellulose fibres will have either fallen into the glass from suspension in the air or been shed by the cloth used to wipe the glass dry.

Note that imperfections of a glass surface can nucleate bubbles: indeed champagne glasses with artificial cavities designed to promote nucleation are available.<sup>11</sup> But in a glass lacking these artificial cavities, cellulose fibres are more numerous and more efficient nucleators of bubbles. No bubbles will form in glass with a smooth surface that has been cleaned with chromic acid solution (which

destroys cellulose and other organic materials).<sup>12</sup>

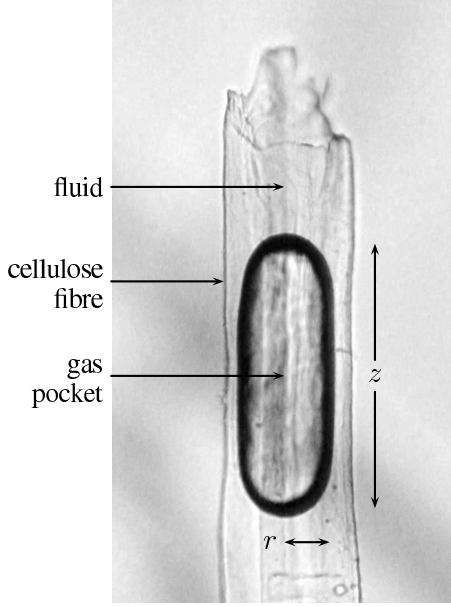


FIG. 1. Geometry of a gas pocket trapped in a cellulose fibre. The fibre is hollow and contains both a trapped gas pocket and fluid.

The mechanism of bubble formation by a gas pocket trapped in a cellulose fibre is illustrated in Figure 2. A cylindrical gas pocket trapped in a cellulose fibre grows by diffusion of dissolved gasses into the pocket. As soon as the pocket reaches the mouth of the fibre it becomes unstable and a bubble breaks off. There are two timescales to the process: the timescale of growth of the gas pocket which is relatively slow and the timescale of detachment of the bubble, which is fast. It is difficult to say exactly how fast the detachment process is. Movies of nucleation events have so far failed to resolve it. The theory presented below<sup>2</sup> predicts the exponential growth of the gas pocket, and the time constant of that exponential growth is taken as an estimate of the bubbling time.

A mathematical model of bubble nucleation by a cellulose fibre can be developed as follows.<sup>2</sup> The rate of change of the amount  $N_1$  (in mol) of carbon dioxide within the gas pocket can be written in terms of fluxes of carbon dioxide through the walls of the fibre,  $Q_W$ , and through the spherical caps at the ends of the gas pocket,  $Q_{SC}$ , as shown in Figure 3,

$$\frac{dN_1}{dt} = 4\pi r^2 Q_{SC} + 2\pi r z Q_W. \quad (5)$$

Two modelling assumptions are used to estimate  $Q_{SC}$  and  $Q_W$ . The first is illustrated in Figure 4, namely that there is a diffusion lengthscale of  $\lambda$  over which the concentration of dissolved carbon dioxide changes from the concentration in equilibrium with the gas pocket  $c_B$

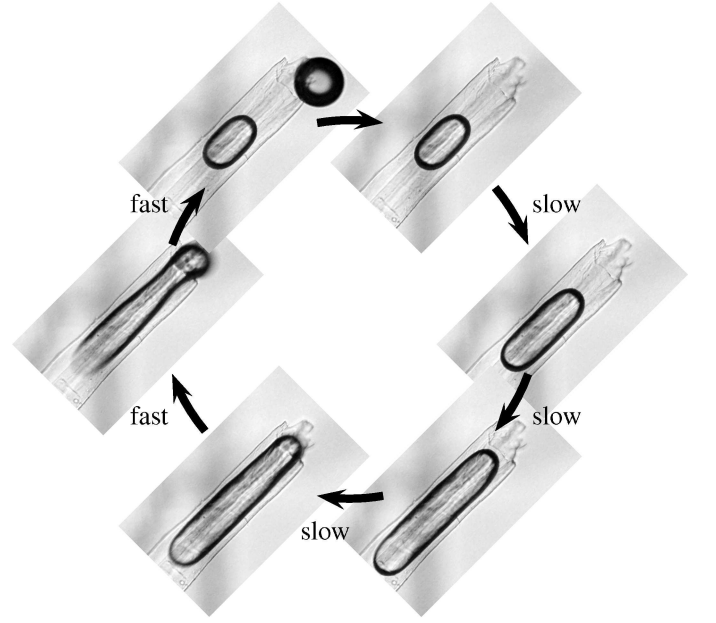


FIG. 2. Nucleation of a bubble by a gas pocket trapped in a cellulose fibre. Although the images taken here are from stout beer, the mechanism is exactly the same in carbonated liquids. The process of bubble formation has two stages: the slow growth of the gas pocket and the fast detachment of a bubble.

to the bulk concentration  $c_1$ .<sup>10</sup> This allows us to estimate

$$Q_{SC} = D_1 \frac{(c_1 - c_B)}{\lambda} = \frac{D_1 H_1}{\lambda} (P_1 - P_B). \quad (6)$$

The diffusion length  $\lambda$  cannot be measured independently so in practise its value is calculated by working backwards from measured nucleation rates.<sup>2</sup>

The second modelling assumption is used to estimate the flux of carbon dioxide through the walls of the fibre. The porous walls of the fibre allow diffusion of carbon dioxide but at a reduced rate.<sup>13</sup> This can be modelled by using the same diffusion length as before and replacing  $D_1$  by  $D_{1\perp} \approx 0.2D_1$ .<sup>2</sup> This allows  $Q_W$  to be estimated as

$$Q_W = D_{1\perp} \frac{(c_1 - c_B)}{\lambda} = \frac{D_{1\perp} H_1}{\lambda} (P_1 - P_B). \quad (7)$$

Substituting the above expressions for  $Q_{SC}$  and  $Q_W$  into equation 5 and using the ideal gas equation,

$$P_B \pi r^2 z = N_1 R T, \quad (8)$$

to rewrite  $N_1$  in terms of  $z$ , the length of the gas pocket, gives

$$\frac{dz}{dt} = \left( \frac{2D_1}{D_{1\perp}} r + z \right) \frac{2RT H_1 D_{1\perp}}{r \lambda} \left( \frac{P_1}{P_B} - 1 \right) \quad (9)$$

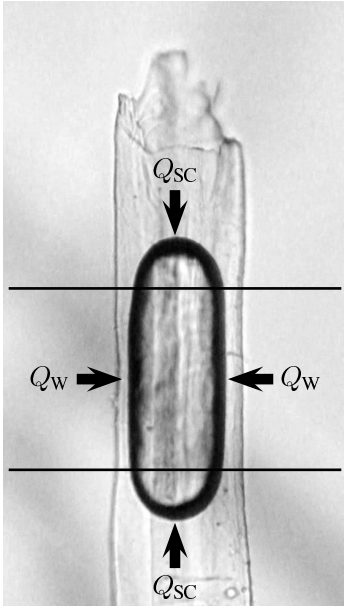


FIG. 3. The rate of growth of the gas pocket can be calculated in terms of  $Q_{SC}$ , the flux of carbon dioxide molecules through the spherical caps at the ends of the gas pocket and  $Q_W$ , the flux through the walls of the cellulose fibre into the gas pocket.

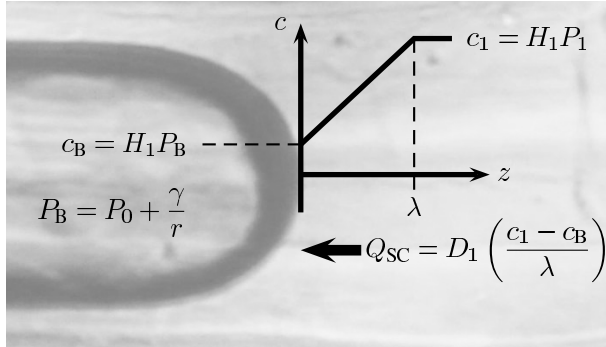


FIG. 4. The diffusion fluxes  $Q_{SC}$  (shown) and  $Q_W$  are estimated by introducing a diffusion length  $\lambda$  over which the carbon dioxide concentration  $c$  varies from the concentration in equilibrium with the gas pocket  $c_B$  to the concentration in the bulk liquid  $c_1$ .<sup>2</sup>

Integrating this equation with initial condition  $z = z_0$

$$z = \left( z_0 + \frac{2D_1}{D_{1\perp}} r \right) \exp\left(\frac{t}{\tau}\right) - \frac{2D_1}{D_{1\perp}} r \quad (10)$$

$$\tau = \frac{r\lambda P_B}{2RT H_1 D_{1\perp} (P_1 - P_B)} \quad (11)$$

where  $\tau$ , the timescale of exponential growth of gas pocket, is also a good estimate of the time to create a bubble.<sup>2</sup> Substituting in values for champagne gives  $\tau = 0.04$  s, and for carbonated beers  $\tau = 0.08$  s.

#### IV. BUBBLES IN STOUT BEERS

There are a number of advantages to using a gas mixture including a large partial pressure of nitrogen in beers. Replacing carbon dioxide with nitrogen changes the taste of the beer and the texture of the head.<sup>1</sup> Unlike carbon dioxide, nitrogen is not acidic in solution, giving stout beers a smoother, less bitter taste. The lower solubility of nitrogen results in smaller bubbles: these give the head of a stout a creamy mouthfeel. The low solubility of nitrogen ensures that the head of a stout beer lasts much longer than that of a carbonated beer.<sup>3</sup>

The small bubble size is responsible for the famous sinking bubbles in stout beers. Drag forces ( $\propto r^2$ ) dominate buoyancy forces ( $\propto r^3$ ) when bubbles are small and so bubbles are dragged downwards at the sides of the glass by the circulation of the beer.<sup>4</sup> A uniform downwards flow of bubbles is unstable and so the bubbles cascade down in waves mathematically equivalent to the roll waves that form in rapidly flowing shallow water.<sup>14</sup>

All the advantages of adding nitrogen come at a price: stout beers do not foam as readily as carbonated beers. The act of poring a carbonated beer is enough to generate a head. This is not the case for stout beers. Special technology is needed to promote foaming in stout beers. In draught form the beer is forced at high pressure through a narrow aperture. In cans widgets are used. A widget is a hollow ball filled with gas at the same pressure as the can. When the can is opened and the headspace depressurises, the widget also depressurises, but can only do so through a small submerged nozzle. The widget releases a turbulent gas jet into the canned beer. The gas jet rapidly breaks up into the hundred million or so bubble nuclei needed to form the head. The stirring of the beer generated firstly by the turbulent jet and secondly by pouring the beer into the glass ensures that the bubble nuclei mix with the beer, scavenging all the dissolved nitrogen and carbon dioxide gasses from solution.

#### V. NUCLEATION OF BUBBLES IN STOUT BEERS

It is interesting to ask why this special technology is needed. The fibre nucleation model developed for carbonated liquids can be adapted for stout beers and used to investigate why the cellulose fibre nucleation mechanism is insufficient to generate a head.<sup>15</sup> The gas pocket in a fibre immersed in stout beer will be at the same total pressure,  $P_B$ , as before, since this only depends on surface tension and geometry. If the amount of carbon dioxide in the gas pocket is  $N_1$  and the amount of nitrogen is  $N_2$  then the partial pressures of carbon dioxide and nitrogen in the bubble will be given by

$$P_{B1} = \frac{N_1}{N_1 + N_2} P_B \quad P_{B2} = \frac{N_2}{N_1 + N_2} P_B, \quad (12)$$



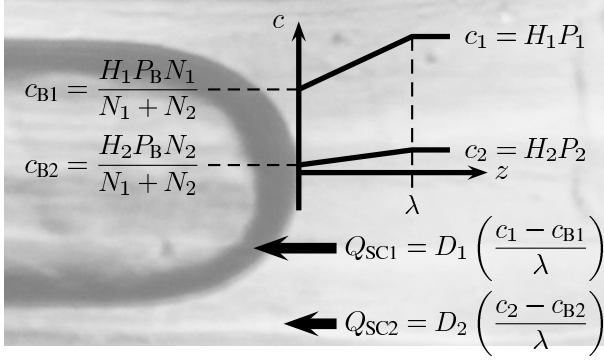


FIG. 5. In a stout beer the rate of growth of a gas pocket in a cellulose fibre depends on the flux of carbon dioxide and nitrogen into the gas pocket. To calculate the flux through the spherical cap we assume as before that there is a diffusion length  $\lambda$  over which the concentrations change from their bulk values to those in equilibrium with the bubble.

corresponding to surface concentrations of

$$c_{B1} = \frac{N_1 H_1 P_B}{N_1 + N_2} \quad c_{B2} = \frac{N_2 H_2 P_B}{N_1 + N_2}. \quad (13)$$

Equation 5 becomes two equations for the rate of change of the amount of carbon dioxide ( $N_1$ ) and nitrogen ( $N_2$ ) in the gas pocket:

$$\frac{dN_1}{dt} = 4\pi r^2 Q_{SC1} + 2\pi r z Q_{W1}, \quad (14)$$

$$\frac{dN_2}{dt} = 4\pi r^2 Q_{SC2} + 2\pi r z Q_{W2}, \quad (15)$$

where  $Q_{SC1}$  and  $Q_{SC2}$  are the fluxes of carbon dioxide and nitrogen through the spherical cap of the gas pocket as illustrated in Figure 5

$$Q_{SC1} = \frac{D_1}{\lambda} (c_1 - c_{B1}) = \frac{H_1 D_1}{\lambda} \left( P_1 - \frac{P_B N_1}{N_1 + N_2} \right) \quad (16)$$

$$Q_{SC2} = \frac{D_2}{\lambda} (c_2 - c_{B2}) = \frac{H_2 D_2}{\lambda} \left( P_2 - \frac{P_B N_2}{N_1 + N_2} \right) \quad (17)$$

The diffusion length  $\lambda$  is assumed to be the same for carbon dioxide and nitrogen.

The fluxes through the wall of the fibre are given by

$$\begin{aligned} Q_{W1} &= \frac{D_{1\perp}}{\lambda} (c_1 - c_{B1}) \\ &= \frac{H_1 D_{1\perp}}{\lambda} \left( P_1 - \frac{P_B N_1}{N_1 + N_2} \right), \end{aligned} \quad (18)$$

$$\begin{aligned} Q_{W2} &= \frac{D_{2\perp}}{\lambda} (c_2 - c_{B2}) \\ &= \frac{H_2 D_{2\perp}}{\lambda} \left( P_2 - \frac{P_B N_2}{N_1 + N_2} \right). \end{aligned} \quad (19)$$

We assume that  $D_{2\perp}/D_2 = D_{1\perp}/D_1 = 0.2$ .

Substituting for the fluxes into equation 14 and 15 gives

$$\frac{dN_1}{dt} = \frac{H_1}{\lambda} (4\pi r^2 D_1 + 2\pi r z D_{1\perp}) \left( P_1 - \frac{P_B N_1}{N_1 + N_2} \right), \quad (20)$$

$$\frac{dN_2}{dt} = \frac{H_2}{\lambda} (4\pi r^2 D_2 + 2\pi r z D_{2\perp}) \left( P_2 - \frac{P_B N_2}{N_1 + N_2} \right). \quad (21)$$

The ideal gas equation

$$P_B \pi r^2 z = (N_1 + N_2) RT \quad (22)$$

is used to eliminate  $z$  leaving

$$\frac{dN_1}{dt} = \frac{H_1}{\lambda} \left[ 4\pi r^2 D_1 + \frac{2D_{1\perp} RT}{r P_B} (N_1 + N_2) \right] \left( P_1 - \frac{P_B N_1}{N_1 + N_2} \right), \quad (23)$$

$$\frac{dN_2}{dt} = \frac{H_2}{\lambda} \left[ 4\pi r^2 D_2 + \frac{2D_{2\perp} RT}{r P_B} (N_1 + N_2) \right] \left( P_2 - \frac{P_B N_2}{N_1 + N_2} \right). \quad (24)$$

### A. Dimensionless Equations

To make further progress we rewrite equations 23 and 24 in dimensionless form using scales

$$N_{\text{scale}} = \frac{2D_2 P_B \pi r^3}{D_{2\perp} RT} \approx 3.22 \times 10^{-13} \text{ mol}, \quad (25)$$

$$t_{\text{scale}} = \frac{r P_B \lambda}{2D_{2\perp} H_2 P_2 RT} \approx 2.73 \text{ s}. \quad (26)$$

The dimensionless equations are

$$\epsilon \frac{dN_1}{dt} = (1 + N_1 + N_2) \left( 1 - \frac{\alpha_1 N_1}{N_1 + N_2} \right), \quad (27)$$

$$\frac{dN_2}{dt} = (1 + N_1 + N_2) \left( 1 - \frac{\alpha_2 N_2}{N_1 + N_2} \right). \quad (28)$$

$N_1$ ,  $N_2$  and  $t$  are now dimensionless variables and

$$\epsilon = \frac{D_2 H_2 P_2}{D_1 H_1 P_1} \approx 0.096, \quad (29)$$

$$\alpha_1 = \frac{P_B}{P_1} \approx 1.45, \quad (30)$$

$$\alpha_2 = \frac{P_B}{P_2} \approx 0.39. \quad (31)$$

Equations 27 and 28 cannot be solved analytically. They can be solved using singular perturbation theory<sup>16</sup> in the asymptotic limit  $\epsilon \ll 1$ . In this limit equation 27 becomes an algebraic equation

$$0 = 1 - \frac{\alpha_1 N_1}{N_1 + N_2}, \quad (32)$$

which can be substituted into equation 28 to give

$$\frac{dN_2}{dt} = \frac{\alpha_1 + \alpha_2 - \alpha_1 \alpha_2}{\alpha_1 - 1} N_2 + \frac{\alpha_1 + \alpha_2 - \alpha_1 \alpha_2}{\alpha_1}. \quad (33)$$

This has the solution

$$N_2 = A \exp\left(\frac{t}{\tau}\right) - \frac{\alpha_1 + \alpha_2 - \alpha_1 \alpha_2}{\alpha_1}, \quad (34)$$

where  $A$  is a constant of integration and

$$\tau = \frac{\alpha_1 - 1}{\alpha_1 + \alpha_2 - \alpha_1 \alpha_2} \approx 0.35, \quad (35)$$

$$\tau t_{\text{scale}} \approx 0.954 \text{ s}. \quad (36)$$

Physically the small epsilon limit assumes that equilibration of carbon dioxide is rapid.

Equations 27 and 28 can be solved numerically. Figure 6 shows the numerical solution with initial conditions  $N_1 = 0$  and  $N_2 = 0.5$ , compared with the asymptotic solution. Fitting the numerical solution for  $5 < t < 10$  to an exponential curve gives a dimensionless bubbling timescale of  $\tau = 0.47$  and a dimensional timescale of  $\tau t_{\text{scale}} = 1.28 \text{ s}$ . In other words the cellulose fibre nucleation mechanism in stout beers is about 15 times slower than in carbonated beers and about 30 times slower than in champagne. This, coupled with the fact that the small bubble size in stout beers means that many more bubbles are needed to make the head, demonstrates why extra technology is needed to form heads on stout beers.

## B. Experimental Observation

The model prediction that cellulose fibres can nucleate bubbles in stout beers can be confirmed experimentally.<sup>15,17</sup> The first ingredient is stout beer containing dissolved gasses. If a canned stout is opened normally, the widget will trigger foaming and the dissolved gasses will end up in the head of the beer, while the beer itself will no longer be supersaturated. To avoid this happening the can must be opened slowly so that the headspace of the can and the widget decompress at similar rates. This will prevent the widget from creating a large number of small bubble nuclei and from stirring the liquid.

One procedure for doing this is to put a small amount of bluetack or other putty-like substance (to create a seal) on the top of the can and then pierce the can through the bluetack with a pushpin. Be careful and wear eye protection while doing so. Allow gas to escape slowly

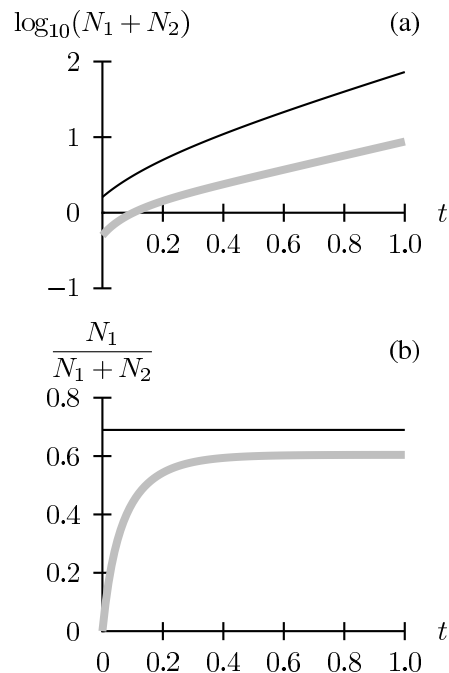


FIG. 6. Asymptotic (black line) and numerical (grey line) solution of equations 27 and 28. (a) Shows the growth of the gas pocket, (b) the mole fraction of carbon dioxide in the bubble. The asymptotic solution assumes that the carbon dioxide in the bubble is in equilibrium with the solution and overestimates the growth rate of the gas pocket.

through the hole: leave the pin in place but enlarge the hole slightly by wobbling it. It should take at least a minute to decompress the can. The pressure in the head space can be monitored by squeezing the sides of the can. Once the head space has reached atmospheric pressure, the pin can be removed. Open the can normally with the ringpull. Extract supersaturated stout beer from the bottom of the can with an eyedropper.

If at this point the can is poured into a beer glass then no head will form and no bubbling will be visible: the beer will be similar in appearance to flat cola. A strong light directed upwards from the base of the glass may reveal a few bubble trains nucleated by (invisible) cellulose fibres.

Figure 7 shows the experimental setup used to visualise bubble nucleation by fibres.<sup>17</sup> Stout beer is carefully (to minimise agitation) transferred into a shallow container in which a source of cellulose fibres has been glued to the base. Laboratory filter paper may be used as the source of the fibres although coffee filter paper works equally well. The fibres are observed through a transmitted light microscope. This setup should be compared with the significantly more sophisticated apparatus needed to investigate bubble nucleation in champagne.<sup>18</sup>

Figure 8 shows several stills from a movie of the nucleation of bubbles by a fibre. If an unusually large fibre is viewed, as in Figure 2 the growth of the gas pocket

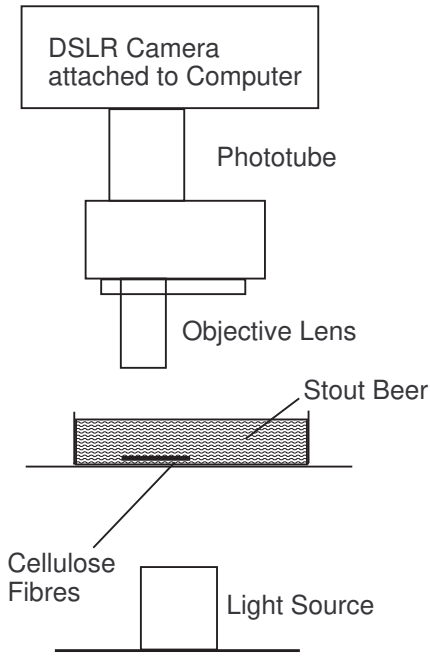


FIG. 7. Experimental setup.<sup>17</sup> Stout beer is poured into a shallow container holding cellulose fibres. The nucleation of bubbles is viewed through a transmitted light microscope. A digital camera is used to record movies of the nucleation events.

and the formation of the bubble can be seen very clearly. The length of the gas pocket ( $z$ ) shown in Figure 2 can be measured as a function of time using edge detection. The results are shown in Figure 9. This shows the steady growth of the gas pocket, as predicted by the model, and the rapid detachment of the bubble (seen as an almost instantaneous contraction of the gas pocket) as assumed by the model.

## VI. APPLICATIONS

One interesting result from the experimental observation of bubble nucleation in stout beers is that it is much easier to study than in carbonated liquids. The experimental setup described above cannot be used to investigate bubble nucleation in carbonated liquids. The larger bubble size typical of carbonated liquids leads to agitation of the liquid, moving the fibres under observation in and out of the plane of focus. Also bubbles in some carbonated liquids rupture into a fine spray of droplets at the surface<sup>19</sup> which coat the objective lens of the microscope, distorting the images. Stout beers therefore are an ideal model system for fundamental research on the fibre nucleation mechanism.

The experimental setup is also accessible for undergraduate laboratory projects. A very minimal set of equipment is needed and good pictures can be obtained

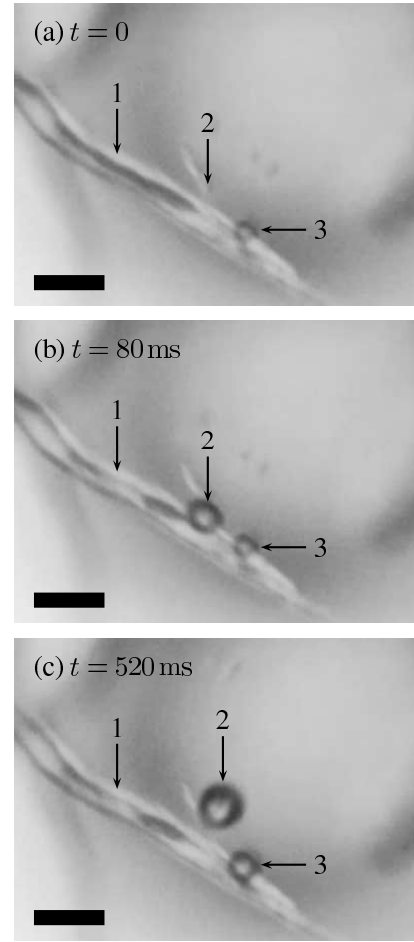


FIG. 8. Nucleation of bubbles observed by the experimental equipment shown in Figure 7. The figures show (1) a gas pocket trapped in the fibre, (2) a bubble created when the air pocket exceeds a critical size, and (3) a bubble growing while attached to the fibre. The scale bar is  $50\ \mu\text{m}$ . (a) The air pocket (1) has just reached critical size. (b) The air pocket (1) has created a bubble (2). (c) Bubble (2) has visibly detached from the fibre.

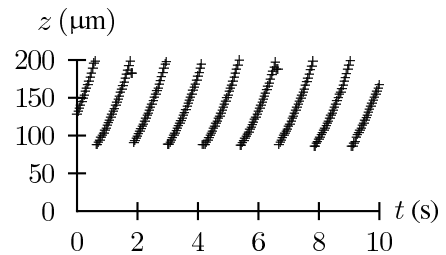


FIG. 9. Plots of length,  $z$ , of the gas pocket shown in Figure 2 as a function of time. The gas pocket grows slowly, then rapidly contracts as a bubble is created.

even with an entry level microscope. Figure 10 shows pictures taken with a usb microscope sold as a promotional item at a local supermarket. The images are good

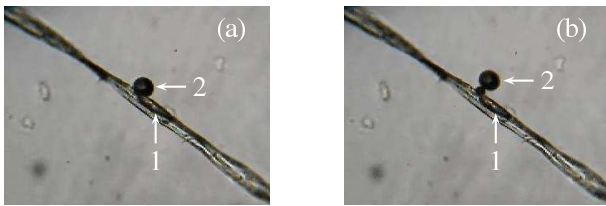


FIG. 10. Images of bubble nucleation in stout beer by cellulose fibres captured with an entry level usb microscope. Despite the unsophisticated equipment, the gas pocket (1) and nucleated bubbles (2) can be visualised.

enough to observe the gas pockets within individual fibres as well as the formation of bubbles. Were it not for the alcoholic nature of the supersaturated solution, these experiments would also be suitable for school science experiments. Unfortunately, as noted above, it is much harder to obtain similar results using carbonated soft drinks.

The fact that cellulose fibres are capable of nucleating bubbles in stout beers leads to the interesting question of whether an alternative widget design based on coating the inside of a bottle or can with fibres would be feasible.<sup>15</sup> The head of a stout beer should contain approximately  $10^8$  bubbles. In order to produce these  $10^8$  bubbles in the 30 s it takes to pour a stout beer from the can into a glass, we require  $4.3 \times 10^6$  fibres (each producing one bubble every 1.28 s). If the fibres are arranged perpendicular to the surface they are attached to, each fibre occupying an area of  $\lambda^2$ , the total area needed is then  $8.3 \times 10^{-4} \text{ m}^2 \approx (3 \text{ cm})^2$ . This rough estimate suggests

such a widget may be feasible.

## VII. CONCLUSIONS

The bubbles in stout beers have a number of extraordinary properties which can ultimately be attributed to the low solubility of nitrogen gas. Stout beers do not foam spontaneously and require special technology to promote foaming, such as the widget found in cans of stout beers. However, theory and experiment shows that the same cellulose fibre nucleation mechanism that causes foaming in carbonated liquids is also active in stout beers, but at a greatly reduced rate. The slow nucleation and growth rate of bubbles makes stout beers an ideal system in which to study nucleation, bringing the study of nucleation within the reach of undergraduate laboratory equipment. In the future, coatings of fibres could be applied to the inside of stout beer cans as a widget replacement. Future research may focus on developing a better understanding of the physics behind the empirical diffusion length  $\lambda$  and the bubble detachment process.

## ACKNOWLEDGMENTS

We acknowledge support of the Mathematics Applications Consortium for Science and Industry (<http://www.macsi.ul.ie>) funded by the Science Foundation Ireland Mathematics Initiative Grant 06/MI/005. MGD acknowledges funding from the Irish Research Council for Science, Engineering and Technology (IRCSET).

\* <http://www.ul.ie/wlee>; [william.lee@ul.ie](mailto:william.lee@ul.ie)

<sup>1</sup> M. Denny, *Froth!: the science of beer* (Johns Hopkins University Press, Baltimore, 2009) 1st. ed.

<sup>2</sup> G. Liger-Belair, C. Voisin, and P. Jeandet, "Modeling non-classical heterogeneous bubble nucleation from cellulose fibers: Application to bubbling in carbonated beverages," *J. Phys. Chem. B*, **109**, 14573–14580 (2005).

<sup>3</sup> C. W. Bamforth, "The relative significance of physics and chemistry for beer foam excellence: Theory and practice," *Journal of the Institute of Brewing*, **110**, 259–266 (2004).

<sup>4</sup> Y. Zhang and Z. Xu, "'Fizzics' of bubble growth in beer and champagne," *Elements*, **4**, 47–49 (2008).

<sup>5</sup> O. A. Power, W. T. Lee, A. C. Fowler, P. J. Dellar, L. W. Schwartz, S. Lukaschuk, G. Lessells, A. F. Hegarty, M. O'Sullivan, and Y. Liu, "The initiation of Guinness," in S. B. G. O'Brien, M. O'Sullivan, P. Hanrahan, W. T. Lee, J. Mason, J. Charpin, M. Robinson, and A. Korobeinikov, editors, *Proceedings of the Seventieth European Study Group with Industry*, 141–182 (2009).

<sup>6</sup> L. D. Landau and E. M. Lifshitz, *Statistical Physics* (Butterworth-Heinemann, Oxford, UK, 1980), 3rd. ed. part 1.

<sup>7</sup> L. D. Landau and E. M. Lifshitz, *Fluid Mechanics* (Butterworth-Heinemann, Oxford, UK, 1987), 2nd. ed.

<sup>8</sup> J. Walker, "Reflections on the rising bubbles in a bottle of beer," *Sci. Am.* **245**, 124–132 (1981).

<sup>9</sup> S. F. Jones, G. M. Evans, and K. P. Galvin, "The cycle of bubble production from a gas cavity in a supersaturated solution," *Adv. Colloid Interface Sci.* **80**, 51–84 (1999).

<sup>10</sup> G. Liger-Belair, M. Vignes-Adler, C. Voisin, B. Robillard, and P. Jeandet, "Kinetics of gas discharging in a glass of champagne: The role of nucleation sites," *Langmuir*, **18**, 1294–1301 (2002).

<sup>11</sup> G. Liger-Belair, S. Villaume, C. Cilindre, and P. Jeandet, "Kinetics of CO<sub>2</sub> fluxes outgassing from champagne glasses in tasting conditions: the role of temperature," *Journal of Agricultural and Food Chemistry*, **57** 1997–2003 (2009).

<sup>12</sup> E. Paynaud, *The Taste of Wine: the Art and Science of Wine Appreciation* (Wine Appreciation Guild, San Francisco, CA, 1987, translated from French by M. Schuster) 1st. ed.

<sup>13</sup> G. Liger-Belair, D. Topgaard, C. Voisin, and P. Jeandet, "Is the wall of a cellulose fiber saturated with liquid whether or not permeable with CO<sub>2</sub> dissolved molecules? Application to bubble nucleation in champagne wines,"



- Langmuir, **20** 4132–4138 (2004).
- <sup>14</sup> M. Robinson, A. C. Fowler, A. J. Alexander, and S. B. G. O’Brien, “Waves in Guinness,” *Phys. Fluids*, **20**, 067101 (2008).
  - <sup>15</sup> W. T. Lee, J. S. McKechnie, and M. G. Devereux, “Bubble nucleation in stout beers,” *Phys. Rev. E* (accepted), arXiv:1103.0508.
  - <sup>16</sup> J. G. Simmonds and J. E. Mann, *A First Look at Perturbation Theory* (Dover Publications, NY, 1998) 2nd. ed.
  - <sup>17</sup> M. G. Devereux and W. T. Lee, “Mathematical modelling of bubble nucleation in stout beers and experimental verification,” *Proceedings of IAENG 2011* (accepted).
  - <sup>18</sup> G. Liger-Belair, M. Parmentier, and P. Jeandet, “Modeling the kinetics of bubble nucleation in champagne and carbonated beverages,” *Journal of Physical Chemistry B*, **110**, 21145–21151 (2006).
  - <sup>19</sup> G. Liger-Belair, “The physics and chemistry behind the bubbling properties of champagne and sparkling wines: a state-of-the-art review,” *Journal of Agricultural and Food Chemistry*, **53**, 2788–2802 (2005).